Melting temperature of fcc metals using empirical potentials

2006 J. Phys.: Condens. Matter 18 8049

(http://iopscience.iop.org/0953-8984/18/34/016)

INSTITUTE OF PHYSICS PUBLISHING JOURNAL OF PHYSICS: CONDENSED MATTER

J. Phys.: Condens. Matter **18** (2006) 8049–8062 doi:10.1088/0953-8984/18/34/016

Melting temperature of fcc metals using empirical potentials

O N Bedoya-Martínez[1], **M Kaczmarski**[1,2] **and E R Hernández**[1]

[1] Institut de Ciència de Materials de Barcelona (ICMAB–CSIC), Campus de Bellaterra, 08193 Barcelona, Spain
[2] Institute of Physics, University of Silesia, Uniwersytecka 4, 40-007 Katowice, Poland

E-mail: ehe@icmab.es

Received 13 April 2006, in final form 26 June 2006
Published 11 August 2006
Online at stacks.iop.org/JPhysCM/18/8049

Abstract

In this paper we present calculations of the zero-pressure melting temperature of a series of face-centred cubic (fcc) metals, including Ag, Rh, Cu, Ir, Au, Pt, Pd, Ni, Al and Pd. Our calculations employed the many-body potential due to Cleri and Rosato (1993 *Phys. Rev.* B **48** 22) to model these systems; in the particular case of Pb, we also employed the 'glue' model of Lim *et al* (1992 *Surf. Sci.* **270** 1109). Melting temperatures were obtained by calculating the Gibbs free energy of the solid and liquid phases, and finding the temperature at which they match. A wealth of other data of interest, ranging from enthalpies of fusion to transport properties, is also reported. Our findings indicate that the models considered in this study account reasonably well for the melting temperature of fcc metals, although there is a tendency to underestimate the experimental values. For the cases of Al and Cu we have also calculated the melting line, up to a pressure of 20 GPa in the case of Al and 100 GPa in the case of Cu.

1. Introduction

The thermal properties of metals, and in particular their melting behaviour, are of great interest in fields as widely varied as engineering, materials processing and geophysics. It is therefore not surprising that there has been considerable effort devoted to characterizing and understanding the thermodynamics of these systems, both experimentally and employing theoretical methods. Experiments, particularly when extreme temperatures and/or pressures are involved, are difficult and costly, but nevertheless over the years a significant amount of data on the melting behaviour of many metals has been accumulated [1, 2]. Concerning theoretical efforts, the calculation of melting data from simulations based on first-principles molecular dynamics (FPMD) methods is becoming the norm, but due to their high computational demands, these calculations are rather costly. While intrinsically less reliable than FP methods, empirical potentials (EP) are still attractive for the study of the thermal behaviour of complex systems, principally for two reasons: firstly, they are computationally much less expensive than

FP techniques, while in some cases affording more than reasonable accuracy; secondly, EP models have frequently been used as 'reference' systems for the calculation of free energies from FP simulations. In such applications, the free-energy difference between the FP model and the EP reference is calculated, and for maximum efficiency and accuracy it is important that the reference system mimics as closely as possible the FP system. Since simulations of the EP model are computationally cheap, its free energy can be evaluated at little cost in a wide range of pressure and temperature conditions.

Another use frequently made of EP models in this context is to chose a given model, and then fit its parameters so that it reproduces as closely as possible data (total energies, forces, etc) obtained from FP simulations. Then the EP model thus constructed is used in large-scale phase coexistence calculations which would be too demanding to perform directly by FPMD. This strategy has been used, for example, by Laio *et al* [3], and by Belonoshko and coworkers [4, 5].

In this general context it is desirable to characterize the different EP models that have been proposed in the literature in their ability to reproduce the thermodynamic behaviour of the materials that they were designed to describe. This has been done, for example for Si employing different models [6–10], for C [11], or for metals employing the modified embedded atom model [12]. In this paper we report results obtained employing the model proposed by Cleri and Rosato [13] to describe a number of fcc metals, including Ag, Rh, Cu, Ir, Au, Pt, Pd, Ni, Al and Pb. For the sake of comparison, this last element has also been simulated with the 'glue' model potential proposed by Lim *et al* [14].

The paper is structured as follows. In section 2 we describe the models employed in this study, and also the computational techniques used. In section 3 we discuss the results obtained for a wide range of properties, such as melting temperatures, enthalpies of fusion, entropies, etc, and finally in section 4 we present the conclusions that are derived from this work.

2. Computational details

2.1. Model

In this work we focus on those fcc metals for which Cleri and Rosato [13] provided a parametrization. These include the metals Al and Pb, and the transition metals Ni, Cu, Rh, Pd, Ag, Ir, Pt and Au. As mentioned above, in the particular case of Pb, we have also used the model of Lim *et al* [14] for comparison. The model of Cleri and Rosato (CR) [13] is based on a second-moment approximation to the tight-binding d-band of transition metals. Properties such as the cohesive energy and structural properties of these systems have been shown to be directly linked to the average value and total width of the d-band, while being relatively insensitive to other features of the band [15, 16]. Hence the assumption that a model having the form of a second-order moment approximation to the tight-binding density of states would work well for transition metals. Although Al and Pb are not transition metals, the same type of model seems to also work for these elements. Cleri and Rosato write the potential energy of the system as

$$U = \sum_i (U_i^R + U_i^B), \tag{1}$$

where the sum is over all atoms in the system, U_i^R is a pair-wise repulsive interaction having the form

$$U_i^R = \sum_j A\mathrm{e}^{-p(r_{ij}/r_0-1)}, \tag{2}$$

where r_0 is the first-neighbour distance in the fcc lattice, and U_i^B is given by

$$U_i^B = -\sqrt{\sum_j \eta^2 \mathrm{e}^{-2q(r_{ij}/r_0-1)}}, \tag{3}$$

which mimics the form of the square root of the second moment of the local density of states, and hence has a many-body character. The parameters A, η, p and q were fitted to experimental values of the cohesive energy, lattice parameters and elastic constants of the systems considered. Cleri and Rosato [13] have shown that this potential is capable of providing enthalpies and volumes of formation of point defects of the parametrized systems in good agreement with experimental results. Likewise, phonon band structures and densities of states are also well reproduced, as are other properties, such as the specific heat, the thermal expansion coefficient, the Grüneisen constant, etc.

The 'glue' model of Lim, Ong and Ercolessi (LOE) [14] is similar in spirit to that of Cleri and Rosato in that it contains both a pair-wise term and a many-body binding term. It has the form

$$U = \tfrac{1}{2}\sum_{j\neq i} V(r_{ij}) + \sum_i F(n_i), \tag{4}$$

where n_i plays the role of a continuous neighbour counter, having the form $n_i = \sum_j \rho(r_{ij})$, where $\rho(r)$ is a monotonically decaying function of r. The LOE model was used by Lim *et al* [14] to study the relative stability of fcc and icosahedral Pb clusters as a function of cluster size, and later the melting of clusters. Both the CR and LOE potentials have been extensively used in simulations of metallic systems in the literature.

2.2. *Methodology*

The determination of coexistence conditions between two phases (e.g. solid and liquid) of a material from computer simulations can be approached in different ways. The most direct, but least accurate, method consists of simulating, via molecular dynamics (MD) or MC, one phase (e.g. the solid phase) along a set of different external conditions, namely different temperatures, until the phase transition sought (in this case melting) is observed. This direct approach has been applied to the study of melting of several metals [17, 13, 18], though it has long been recognized that such a method can only provide an upper bound to the *theoretical* equilibrium melting temperature, i.e. the melting temperature predicted by the model (which is, in general, different from the experimental melting temperature). This occurs because the kinetics of first-order phase transitions are subject to hysteresis effects, which in turn are affected by a number of factors, such as the presence (or absence) of defects, surfaces, the system size, etc. The influence of these factors is negligibly small in macroscopic samples, but not so in computer simulations, where the size of the system is always small compared to experimental bulk samples. Therefore the errors committed in the estimation of the coexistence conditions using this direct approach can be severe. Furthermore, these errors are impossible to dissociate from the intrinsic limitations of the model used to simulate the system. Recently, Laio and Parrinello [19] and Martoňák *et al* [20] have proposed a scheme which, in principle, avoids hysteresis effects, and which has been used to model solid–solid phase transitions in silicon [20], and more recently has also been employed to study the perovskite to post-perovskite phase transition in $MgSiO_3$ [21].

An alternative approach, which we have actually employed in the majority of the calculations reported here, consists of evaluating, for each phase α and β of the material, the free energies G_α and G_β as a function of the external conditions, temperature T, and/or pressure P. Thus we can find the conditions where $G_\alpha(T, P) = G_\beta(T, P)$, i.e. where the two phases are in equilibrium with each other. More details of our computational procedure are given below.

Finally, there is a third method, sometimes referred to as the two-phase method, in which the two phases are simulated in direct coexistence, with an interface separating them. If this

combined system is simulated in microcanonical (constant N, V and E) conditions, then, after some readjustment of the relative numbers of atoms in each phase, the temperature will oscillate around the coexistence value. Alternatively, the system can be monitored in isothermal–isobaric (constant N, P, T) conditions. Then, if the temperature is fixed at some value below the melting temperature, the liquid will eventually solidify, leaving only the crystalline phase behind. Conversely, if the external temperature is fixed above the melting temperature, the solid phase will eventually melt. By repeating this process one can effectively bracket the coexistence temperature with the required accuracy. This method has been employed regularly for calculating melting temperatures of materials using empirical potentials, such as in the case of Si [7, 8, 22]. More recently, it has even been used at the level of first-principles simulations [23, 24], though its use in this context is extremely demanding of computational resources, given the need of simulating many hundreds or even thousands of atoms. We have used the two-phase technique in one particular case, discussed below, to compare with the results of the free-energy-based approach.

The computational techniques used in this study are the same as those employed in our earlier studies on silicon [9, 10], and a detailed description has been provided elsewhere [9], therefore here we will just provide an outline of our computational strategy. In order to locate the melting transition, we start by evaluating the free energy of the solid phase at some reference temperature, T_s, and likewise for the liquid, at temperature T_l, where T_s and T_l are chosen so that they bracket from below and above, respectively, the melting temperature sought. The free energy is obtained for each phase by choosing an appropriate reference system for which the free energy is known, and computing the free-energy difference between the reference and the system of interest. In the case of the solid phase we have employed the Einstein solid as reference, for which the free energy can be calculated analytically, while in the case of the liquid phase we have used the Lennard-Jones fluid, for which the free energy has been tabulated by Johnson *et al* [25]. The free-energy difference between the reference and the system of interest is computed from an *adiabatic switching* MD calculation in NVT conditions, following Watanabe and Reinhardt [26]. In an adiabatic switching calculation, the reference system is slowly (quasi-adiabatically) converted into the system of interest (or vice versa) during the course of a single, non-equilibrium simulation. In so doing, the work consumed in the process is accumulated. In the adiabatic limit this work would be exactly equal to the free-energy difference between the system of interest and the reference, but in simulations this limit can only be approached, but not strictly attained. Therefore the accumulated work contains a dissipative contribution, and hence the work is an upper bound to the free-energy difference (or a lower bound if the transformation starts at the system of interest and ends at the reference). Experience shows, however, that sufficiently well-converged values of the free-energy difference can be obtained within typical simulation runs (a few picoseconds or tens of picoseconds long).

We then employ the *reversible scaling* technique [27] in NPT conditions [28] to calculate the free energy of both solid and liquid phases in the range of temperatures $[T_\mathrm{s}, T_\mathrm{l}]$. The reversible scaling technique is very similar to adiabatic switching, but instead of calculating the free-energy difference between two different systems (target and reference), it allows one to calculate the free-energy difference between the target system at temperature T, and the same system at a reference temperature, T_0, at which the free energy is known (has been previously calculated). This technique exploits the formal thermodynamic equivalence between scaling the potential energy by a factor λ and scaling the temperature by a factor λ^{-1}. If the λ parameter scaling the potential energy is varied between $[1, \lambda_\mathrm{f}]$ during the course of the simulation, then the free energy is obtained between temperatures T_0 and T_0/λ_f, where T_0 is the temperature at which the reversible scaling simulation is conducted. By performing this

kind of simulation for both the solid and liquid phases, we can locate the temperature at which $G_s = G_l$, which is by definition the coexistence, or melting temperature, T_f. As a check to this procedure, we subsequently evaluate the free energy of each phase at the estimated value of T_f, employing the same procedure as for the reference temperatures T_s and T_l. Naturally, these free energies should again be equal, but the adiabatic switching and reversible scaling calculations are subject to small errors which will cause these free energies to be not exactly the same. Their discrepancy should nevertheless be small, and allows us to quantify the error bars in our estimated value of T_f. From these calculations, we also obtain as a by-product the enthalpy of fusion, ΔH_f, and the equilibrium volume of the solid and liquid phases at coexistence, quantities from which we can infer, through the Clausius–Clapeyron equation, the value of dT_f/dP, the pressure derivative of the melting line. In separate simulations, we also obtain average structural and dynamical properties of each phase, such as radial distribution functions, diffusion coefficients, etc.

In some specific cases, namely those for which the potentials used in this work provide better agreement with the experimental value of dT_f/dP, we have also calculated the melting curve using the *dynamical Clausius–Clapeyron integration technique* [28]. The dynamical Clausius–Clapeyron integration technique is an extension of the reversible scaling method, which allows us to obtain the coexistence line between two phases starting from given conditions of T and P where they are known to be in equilibrium. Starting at these conditions, the two phases are simulated in parallel, but in separate simulation boxes (i.e. without an interphase). Following the same procedure as in the reversible scaling technique, the two phases are simulated at constant temperature T_0, but the potential energy is scaled by λ in such a way that effectively the temperature varies from T_0 to T_0/λ_f in a quasi-continous fashion. At each λ value, the Clausius–Clapeyron equation is used to calculate the corresponding change in the pressure variable.

In all our simulations we have used systems consisting of 500 atoms in periodic boundary conditions. We have conducted tests to establish the sensitivity of the calculated melting temperatures on the size of the system which indicate that these values converge very rapidly with the number of atoms considered in the simulations. In fact, sizes of the order of 100 atoms are quite sufficient for the present purpose, but we have settled on the larger size because the models employed are computationally undemanding, and in this way we minimize the statistical uncertainty in other computed quantities, such as fusion enthalpies, molar volumes, etc. The system is coupled either to a Nosé–Poincaré thermostat [29] or, in the case of adiabatic switching and reversible scaling simulations, to the stochastic thermostat of Andersen [30]. Constant-pressure conditions, when needed, are imposed using the scheme of Souza and Martins [31] as implemented by one of the present authors [32]. All our calculations have been carried out using the Trocadero code [33].

3. Results and discussion

3.1. Melting and thermodynamic properties

Following the procedure outlined above, we have obtained the zero-pressure melting point for Ni, Cu, Rh, Pd, Ag, Ir, Pt, Au, Al and Pb modelled using the CR potential. For the latter element, the calculation was repeated employing the LOE potential.

Figure 1 shows the calculated free energies of solid and liquid Pb as predicted by the CR and LOE potentials, in the vicinity of the melting point. It can be seen that, according to the CR model, the free energies match at 466 K, which is therefore the melting point of Pb predicted by this potential. This falls somewhat below the experimental value of 600.1 K [34], an error of

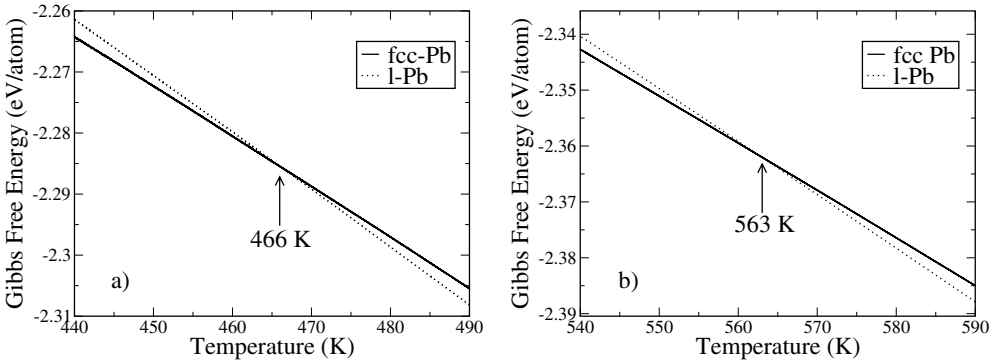

Figure 1. Free energy of the solid and liquid phases of Pb as a function of temperature, calculated using (a) the CR [13] potential, and (b) the LOE [14] potential.

Table 1. Melting temperatures of fcc metals at zero pressure. The first column lists our calculated values, which are compared to those calculated by other authors, listed in the second column, and to experimental values in the third. Experimental values were taken from [34].

	T_f (This work) (K)	T_f (Other calc.) (K)	T_f^{exp} (K)
Ag	1033 ± 15	907 ± 15[a], 1330[b]	1234.93
Rh	2678 ± 71	1763 ± 29[a]	2237.15
Cu	1237 ± 7	1073 ± 17[a], 1490[b], 1176 ± 100[c]	1357.77
Ir	3292 ± 52	2124 ± 35[a]	2719.15
Au	927 ± 37	1159 ± 19[a]	1337.33
Al	870 ± 5	890 ± 20[d], 912 ± 50[e]	933.47
Pb_{CR}	466 ± 5	625 ± 10[a]	600.61
Pb_{LOE}	563 ± 1	598[f]	600.61
Pt	1579 ± 78	1794 ± 29[a]	2041.55
Pd	1257 ± 92	1215 ± 20[a]	1828.05
Ni	1796 ± 2	1359 ± 22[a], 1880[b]	1728.15

[a] From [18]. [b] From [13]. [c] From [35]. [d] From [36]. [e] From [37]. [f] From [14].

-22%. The LOE model seems to fare better, as it gives a melting temperature of 563 K, much closer to the mark (an error of -6%). Lim and coworkers [14] estimated a melting temperature of 598 K by extrapolating the melting temperatures of Pb clusters of different sizes to the infinite size limit. Although this value is close to the experimental result, it is probably subject to a large uncertainty, given that it was obtained from an extrapolation (the largest cluster size considered by Lim *et al* was 2057 atoms, for which the melting temperature was found to be close to 500 K). Nevertheless the agreement between both calculated values is good, and we can conclude that, at least for the case of Pb, the LOE potential gives a better description at temperatures close to the melting point than the CR model.

In table 1 we list our calculated values for the melting temperatures, comparing with results from other calculations and with experimental values. In table 2 we list the enthalpies of fusion, ΔH_f, entropies of fusion, ΔS_f, fractional volume change, $\Delta V/V_s$, and slope of the melting line at zero pressure, dT_f/dP. Whenever possible, experimental data and other theoretical predictions are given for comparison.

Except in the cases of Ni, Rh and Ir, for which we obtain melting temperatures that fall above the experimental value, our calculated melting temperatures fall slightly below the

Table 2. Thermodynamic properties of fcc metals at the melting point.

	ΔH_f (eV/atom)	ΔS_f (k_B)	$\Delta V/V_s$ (%)	dT_f/dP (K GPa^{-1})
Ag	0.101 (0.117[a])	1.212 (1.164[b])	6.1 (3.8[e])	72.35 (64.7[b])
Rh	0.352 (0.276[a])	1.414	11.06 (12.0[f])	82.27 (61.7[f])
Cu	0.133 (0.134[a])	1.108 (1.157[b])	6.06 (4.2[e])	45.18 (41.8[b])
Ir	0.436 (0.426[a])	1.560	10.70	79.30
Au	0.101 (0.132[a])	1.350 (1.164[b])	6.79 (5.1[e])	70.60 (57.0[b])
Al	0.084 (0.112[a])	1.103 (1.38[c])	4.15 (6.5[e])	47.7 (65[g], 43[h])
Pb_{CR}	0.049 (0.050[a])	1.292 (1.027[d])	5.31 (3.5[e])	99.8 (82.0[i])
Pb_{LOE}	0.053	1.190	2.92	59.71
Pt	0.180 (0.230[a])	1.472 (1.158[d])	7.06 (7.0[f])	62.73 (71.5[f])
Pd	0.138 (0.173[a])	1.410 (1.133[d])	7.10	64.50
Ni	0.209 (0.177[a])	1.421 (1.224[d])	8.88 (4.5[3])	57.73 (41.8[f])

[a] From [34]. [b] From [46]. [c] From [47]. [d] From [48]. [e] From [1]. [f] From [49]. [g] From [44]. [h] From [45]. [i] From [50].

experimental values. In the cases of Rh and Ir, the overestimation is substantial (441 K in the case of Rh, and 573 K in the case of Ir) and is probably due to either poorer fitting of the model in these particular cases, or to larger uncertainty in the experimental values used in the fitting of the potential. In the case of Ni, there is also an overestimation of the experimental melting temperature, but much smaller (68 K) than in the cases of Rh and Ir. In fact, the smallest discrepancy is found in the case of Ni. Also, for Al the discrepancy is rather small, with our predicted melting temperature within 70 K of the experimental value (an error of -7%), but more typical discrepancies are around 20%, with a general tendency to underestimate, except in the noted cases of Ni, Rh and Ir. There could be several reasons for the discrepancies seen in the cases of Ni and Rh; possibly the quality of the experimental data to which the CR model was fitted in these cases was lower, or the fitting procedure was less accurate.

Once the melting temperature of each metal was determined as explained above, we conducted further simulations at the predicted melting temperature in NVT conditions. These simulations had the purpose of analysing the validity of the Lindemann [38] melting criterion in the case of the solid phase, while those conducted in the liquid phase allowed us to determine the transport coefficients, and we discuss those results below (see section 3.2).

There has been a long effort in the scientific community directed at understanding how melting actually occurs [39]. In particular, there have been several attempts to correlate the occurrence of melting with some thermally dependent feature of the solid. One such attempt is the well-known Lindemann [38] melting criterion, which establishes that a solid melts when the amplitude of the thermal motion of the atoms around their equilibrium positions reaches a critical fraction of the nearest-neighbour distance. Another well-known melting criterion is that due to Born [40], according to which melting occurs once the crystal loses its rigidity, i.e. when its shear modulus vanishes. Recently, these two melting criteria have been shown to be equivalent at the limit of superheating [41] (mechanical melting). At equilibrium melting, the liquid nucleates at surfaces and defects, propagating to the rest of the crystal. In these melting nuclei, the thermal oscillations of atoms have higher amplitude (typically around 20% of δ, the nearest-neighbour distance) than bulk crystal atoms (which have amplitudes of the order of 10% of δ). When mechanical melting occurs, i.e. when the shear modulus of the crystal goes to zero, all atoms are found to oscillate with amplitudes corresponding to the values observed in melting nuclei in equilibrium melting [41].

At the melting temperature calculated for each metal, we have measured the average displacement amplitudes, which range from 11.5% to 13.6% of the nearest-neighbour distance.

While there is some scatter in the results, they seem to indicate that indeed, for the fcc metals considered here, there is a critical value of the atomic displacements beyond which melting occurs. Martin and O'Connor [42] have measured experimentally the vibrational amplitudes of a series of materials close to their melting points, and concluded that the Lindemann criterion is applicable in materials of a similar kind. They found that, in the case of fcc metals Al and Cu, the amplitude of the thermal vibrations reached 8% of the nearest-neighbour distance close to the melting temperature. In the case of alkali halides, the value was closer to 11%. The values we obtain for the fcc metals are somewhat larger than those reported by Martin and O'Connor, which could be due to the fact that their measurements were taken at temperatures close to, but below, the melting temperature, but are more likely to be a consequence of the model.

The melting of fcc metals has previously been studied by several authors with the same or similar models to those used here. Cleri and Rosato [13] considered, in particular, the cases of Ni, Ag and Cu, while Gómez *et al* [18] modelled the melting of all metals considered in this study, but with a slightly modified version of the CR potential. Let us first comment on the comparison of our calculated melting temperatures with those obtained by Cleri and Rosato (who only considered the cases of Ni, Ag and Cu) using the same model. Cleri and Rosato used what we have referred to in section 2.2 as the direct method, namely, simulating the solid in *NPT* conditions at different temperatures until the system was observed to melt. As has already been commented, this procedure invariably results in an overestimation of the theoretical melting temperature. Their results for these systems are of the order of 300 K higher than ours for Rh and Cu (84 K in the case of Ni) and, since their simulations were also carried out for systems of 500 atoms, this discrepancy cannot be attributed to different size effects. We therefore conclude that the difference between their estimated melting temperatures and ours is a manifestation of the hysteresis effects in the results of Cleri and Rosato. Furthermore, their results are invariably higher than the experimental values (typically by 100–200 K), while the ones that we obtain, both for the same metals and for those for which Cleri and Rosato did not estimate the melting temperature, are generally below the experimental values (with the noted exceptions of Rh and Ir). Gómez *et al* [18] also used the direct method to estimate the melting temperatures of fcc metals, so it is also likely that their results provide overestimations of the true melting temperatures as predicted by their model. Unfortunately, they used a somewhat simplified version of the CR potential, and therefore their results are not directly comparable to those of Cleri and Rosato, nor to those obtained in this study. Indeed, it is striking that, in the cases of Ni, Ag, and Cu (the three cases for which Cleri and Rosato estimated the melting temperature), the results of Gómez *et al* are, on average, nearly 400 K below those obtained by Cleri and Rosato. Furthermore, with the only exception of Pb, Gómez *et al* predict melting temperatures that are several hundreds of K below the experimentally measured melting temperatures. Therefore it can be expected that the true melting points of the CR model, as modified by Gómez *et al*, fall significantly below the experimental melting temperatures.

The melting of Al has been calculated from first-principles simulations in different ways [36, 43, 37, 23]. In the work of de Wijs *et al* [36] the melting of Al at zero pressure was calculated by obtaining the free energy of the fcc and liquid phases directly from density functional theory (DFT) simulations. They reported a melting temperature of $T_m = 890 \pm 20$ K, which is in very good agreement with the experimental value, and also very close to the result that we obtain with the CR potential. According to the results of de Wijs *et al*, the value of dT_m/dP is very close to the experimental result of Cannon [44], which is 65 K GPa^{-1}. The CR potential, on the other hand, gives a result of 49.2 K GPa^{-1} (see table 2), which is further away from the value reported by Cannon, but closer to the value recently obtained by Hänström and Lazor [45] (43 K GPa^{-1}). We can therefore conclude that both first-principles methods and

the CR potential predict values of the slope of the melting line which are within experimental uncertainty bounds. Jesson and Madden [43] also estimated the melting temperature of Al following the same procedure as de Wijs *et al* [36]. However, they employed an orbital-free functional instead of using the Kohn–Sham ansatz of DFT. They obtained a rather low melting temperature, 615 K, more than 300 K below the experimental value. More recently, Vočadlo and Alfé [37] have calculated not only the zero-pressure melting point, but even the melting curve up to pressures of 150 GPa. These authors used a generalized-gradient functional form for the exchange and correlation energy in DFT, and obtain a melting temperature of 786 ± 50 K, which they corrected to a new value of 912 ± 50 K when taking into account the overestimation of the equilibrium lattice parameter of Al committed by the exchange–correlation functional employed in their calculations.

Vočadlo *et al* [35] have calculated the melting line of Cu up to 100 GPa from two-phase simulations employing an empirical potential fitted to first-principles simulations. At zero pressure, they obtain a melting temperature of 1176 ± 100 K, which is in good agreement with our result. For the pressure derivative at zero pressure, they give a value of 38 K GPa^{-1}, which is again in good agreement with the value that we obtain (see table 2) and also with experimental results.

In order to double-check our estimations of the melting temperature by means of free-energy calculations, we have also sought to determine it by an alternative method, namely the two-phase approach, described in section 2.2. We have chosen the case of Pb, as modelled with the CR potential for this check. The system was prepared as follows: a simulation box containing 500 atoms of the fcc solid phase was equilibrated at temperatures between 400 and 500 K at regular intervals of 20 K, employing *NPT* MD simulations with $P = 0$ GPa. These simulations provided the average lattice parameter at each temperature. The liquid phase was then prepared in a box also containing 500 atoms, having two sides of equal length to that of the fcc phase at the same temperature, while the third length was free to adapt to the external pressure. We then proceeded to join the two phases together in a single simulation box, with the interface parallel to a [100] plane in the fcc solid. After putting the two phases together, a short simulation was carried out with the atoms in the solid phase frozen, in order to allow the liquid to adapt to the presence of the solid. With the system thus prepared, we conducted long (200 ps) in *NPT* conditions, where the three sides of the simulation cell were allowed to evolve independently, but the angles α, β and γ were constrained at 90°. During these simulations, the system was observed to evolve until only one phase (solid or liquid) prevailed (see figure 2). At all temperatures up to 480 K, the system was observed to freeze into the solid phase, while it eventually melted at 500 K. We then performed a final simulation at 490 K, where again the system was observed to melt (see figure 2(b)). Thus, our two-phase simulations indicate that the melting of fcc Pb according to the CR potential is to be found between 480 and 490 K. This is in good agreement with our previous result based on free-energy calculations (466 ± 6 K), though in principle outside of the upper bound of the error bar of the free-energy calculation. In order to clarify the reasons for this slight discrepancy, we have re-calculated the melting temperature of Pb using the free-energy approach employing different system sizes. In particular, we have considered systems containing 64, 108, 256 and 864 atoms, as well as our standard system size of 500 atoms. The values obtained are 480 ± 28 K (64 atoms), 476 ± 14 K (108 atoms), 478 ± 13 K (256 atoms), and 479 ± 14 K (864 atoms). These values agree with each other within the error bars, and are also in excellent agreement with the value deduced from the two-phase simulations. It seems that the value originally calculated with 500 atoms is slightly (10–15 K) below the trend; this is most likely due to the fact that the range of temperatures $[T_s, T_l]$ used to bracket the melting temperature T_f in this case was wider, since initially the actual value was unknown. In any case, we take the view that the two results are sufficiently close to one

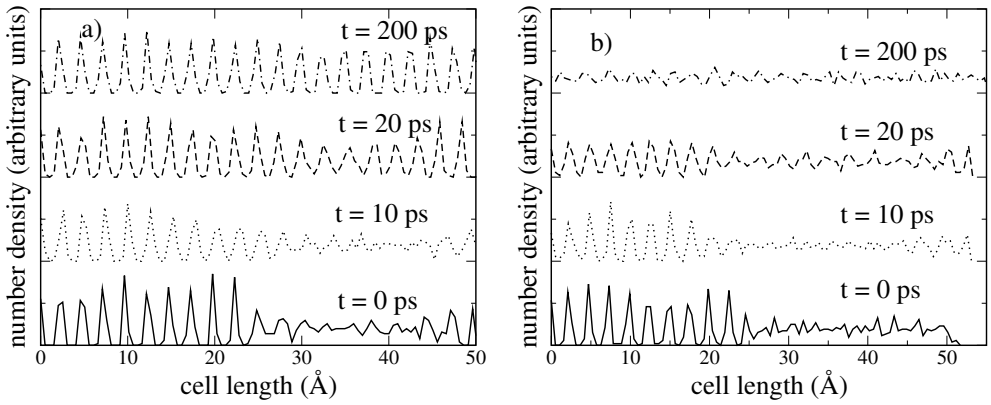

Figure 2. Two-phase simulations of Pb with the CR potential. The plots show the number density of the system along a line perpendicular to the interface as a function of time. The density spikes to the left of the curve at the start of the simulations correspond to planes of atoms in the crystal, while the homogeneous density on the right corresponds to the liquid phase. The left panel (a) shows the density evolution at 440 K, where, as time progresses, the solid phase eventually occupies the whole simulation cell. On the right side (b), at 490 K, it is the liquid phase that ends up filling the system.

another, and to the value obtained with the two-phase simulations, that we can consider them to be in good agreement.

Regarding enthalpies of fusion (see table 2), again we note a slight tendency to underestimate the experimental value, except in the cases of Ni, Rh and Ir, where there is an overestimation, consistent with the fact that these are the three elements for which the CR potential overestimates the melting temperature. We therefore conclude that the CR parametrization tends to stabilize the liquid with respect to the solid phase, which results in low melting temperatures. The entropies of fusion are generally small, typically 1.1–1.2 k_B, and our calculated values are in good agreement with the experimental values, with a slight tendency to overestimate.

Another important quantity is the pressure derivative of the melting line at zero pressure. The ability of a model to correctly reproduce this value provides an indication of how well the model is likely to describe the melting line. We notice that the CR potential gives a value of dT_m/dP which is, in general, within 30% of the experimental value, when the latter is known. We have chosen the cases of Cu and Al, for which the discrepancy between calculated and experimental values of dT_m/dP is among the smallest, to calculate the melting line by integration of the Clausius–Clapeyron equation, following the method of de Koning *et al* [28]. Our calculated melting lines are shown in figure 3. In order to check the correctness of the calculated melting line at finite pressures, we independently evaluated the melting temperature at pressures of 5 and 20 GPa (results indicated by filled circles in figure 3) and, as can be seen, the melting line and these calculated finite pressure melting points are in mutual agreement. For the case of Al, although our calculated melting temperature at zero pressure is in good agreement with the experimental results of Hänström and Lazor [45] and Boehler and Ross [51], as well as with the calculated values of de Wijs *et al* [36] and Vočadlo and Alfè [37], it is clear that the value of the pressure derivative of the melting temperature predicted by the CR model (49.2 K GPa^{-1}; see table 2) is too small, as our calculated melting line deviates from the experimental and *ab initio* data as the pressure is increased. Because of this, we have not attempted to obtain the melting line beyond pressures of 20 GPa. In the case of Cu, the agreement of the melting temperature at zero pressure is a bit poorer than in the case of Al,

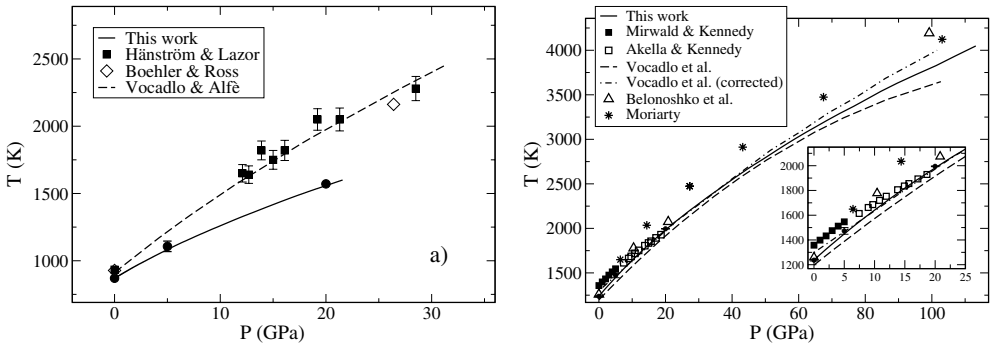

Figure 3. Melting line of (a) Al and (b) Cu, calculated using the dynamical Clausius–Clapeyron integration method of de Koning *et al* [28]. We compare our results with the work of Hänström and Lazor [45], that of Boehler and Ross [51], and that of Vočadlo and Alfè [37] in the case of Al, and that of Mirwald and Kennedy [46], Moriarty [52], Vočadlo *et al* [35], and Belonoshko *et al* [5] in the case of Cu.

with an underestimation of about 120 K, but on the other hand the predicted value of $\mathrm{d}T_\mathrm{f}/\mathrm{d}P$ is closer to the experimental value (see table 2), and therefore agreement with the experimental and *ab initio* data is reasonable, even at pressures as high as 100 GPa.

3.2. Transport properties

Transport properties of liquid metals, such as the diffusion coefficient and viscosity, are both of practical and fundamental interest. From a technological point of view, the processing of liquid metals for alloying, glass formation and other engineering processes requires the knowledge of transport properties. At a more fundamental level, universal scaling laws of transport coefficients have been proposed [53–55], and there is evidence from simulation that liquid metals adhere to these scaling laws particularly well [56, 57]. Transport properties of liquid metals have been studied before with computer simulations on a number of occasions, though not normally at the melting temperature, since usually the latter was not determined in the same study. Hence we report here the diffusion coefficient and viscosity for each metal in the liquid state at the melting temperature predicted by the model.

In order to determine the transport properties of each liquid metal at its corresponding melting temperature, we have performed NVE MD simulations at the volume of the liquid phase and at the calculated melting temperature. The diffusion coefficient, D, was obtained from the slope of the mean-squared displacements in the standard way. The viscosity, μ, was estimated from the Stokes–Einstein relation, $D\mu = k_\mathrm{B}T/2\pi a$, where a is an effective atomic diameter. Strictly speaking, this relation is only valid for Brownian motion, but it has been shown [58] to work reasonably well for atoms if a is chosen to be equal to the position of the first peak in the radial distribution function. In the case of the metals considered here, this procedure has been shown to lead to results essentially indistinguishable from those provided by the more appropriate Green–Kubo relation [59].

The diffusion coefficient, D, and viscosity, μ, of the liquid metals considered in this study have been previously obtained by Alemany and coworkers [59] using the CR potential, at temperatures slightly above the experimentally measured ones for each case. Consequently, their values of D and μ correspond to higher temperatures than our own, and hence it is not surprising that their calculated diffusion coefficients are somewhat larger than those we obtain. Since we estimate the viscosity from the Stokes–Einstein relation, our values are a little

Table 3. Diffusion coefficient and viscosity (obtained from the Stokes–Einstein relation) for the molten metals considered in this study. The experimental data for the diffusion coefficient were calculated at the experimental melting temperature employing the fitting expressions given in [1].

	$D \times 10^5$ (cm^2 s^{-1})			η (m Pa s)		
	This work	Ref. [59]	Exp. [1]	This work	Ref. [59]	Exp. [1]
Ag	1.90	2.65	2.54	4.24	3.70	3.88
Rh	3.96	—	—	5.02	—	—
Cu	2.72	2.72	3.97	4.03	4.33	4.00
Ir	2.58	—	—	10.58	—	—
Au	1.54	2.60	—	4.76	3.93	5.00
Al	4.00	4.68	—	1.76	1.60	1.30
Pb_{CR}	1.02	1.33	0.17	2.97	3.20	2.65
Pb_{LOE}	1.20	—	—	3.17	3.20	2.65
Pt	1.97	2.81	—	6.60	6.17	—
Pd	2.42	4.03	—	4.30	3.68	—
Ni	3.70	2.52	—	4.40	5.85	4.90

higher than those obtained by Alemany *et al*. Nevertheless, their results and ours are mutually consistent, bearing in mind this temperature difference, which in some cases can be as large as several hundred degrees. Our calculated values of D and μ are compared with the theoretical values of Alemany *et al* [59] and with experimental values in table 3. Comparing with the experimental values of the diffusion coefficient, which seems to be known only for Ag, Cu and Pb, agreement is reasonable for Ag and Cu, but the experimental value for Pb seems to be rather low, more so if we take into account the good agreement between the calculated value of Alemany *et al* [59] and our own. In fact, the experimental value for D seems to be inconsistent with the experimental value of μ, if one asumes the validity of the Stokes–Einstein relation; hence we conclude that the experimental D value is a significant underestimation.

In 1996 Dzugutov [55] proposed a universal relation linking the diffusion coefficient and the excess entropy, i.e. $S - S_{\mathrm{id}}$, where S_{id} is the entropy of the ideal gas at the same density and temperature. Dzugutov found, via molecular dynamics simulations, that the diffusion coefficients calculated in many different systems followed very closely a relation having the form $D^* = 0.049\mathrm{e}^{(S-S_{\mathrm{id}})}$, where D^* is a scaled dimensionless form of the diffusion coefficient, $D^* = D\Gamma^{-1}\sigma^{-2}$. Here σ is the position of the first maximum in the radial distribution function, and Γ is the collision frequency of an atom with the sphere of its first neighbours. According to Enskog's theory, this is given by $\Gamma = 4\sigma^2 g(\sigma)\rho\sqrt{\pi k_{\mathrm{B}}T/m}$, where $g(\sigma)$ is the peak value of the radial distribution function, ρ is the number density, k_{B} is Boltzmann's constant, and m is the mass of the atoms. In fact, Dzugutov used the so-called two-particle approximation to the excess entropy,

$$S - S_{\mathrm{id}} \approx S_2 = -2\pi\rho \int_0^\infty \left\{ g(r) \ln\left[g(r)\right] - \left[g(r) - 1\right] \right\} r^2 \, \mathrm{d}r. \tag{5}$$

Later Hoyt *et al* [56] and more recently Li *et al* [57] have corroborated and extended the observations of Dzugutov [55]. Since we have calculated the diffusion coefficients in the liquid phase at melting, and we have also obtained the entropy at that temperature, we can automatically check how consistent are our results with Dzugutov's universal relation. In figure 4 we plot our calculated diffusion coefficients, where they are compared with Dzugutov's prediction. Although obviously there is some scatter in the data, it is clear there that our calculated values of the diffusion coefficient are consistent with the universal behaviour found by Dzugutov.

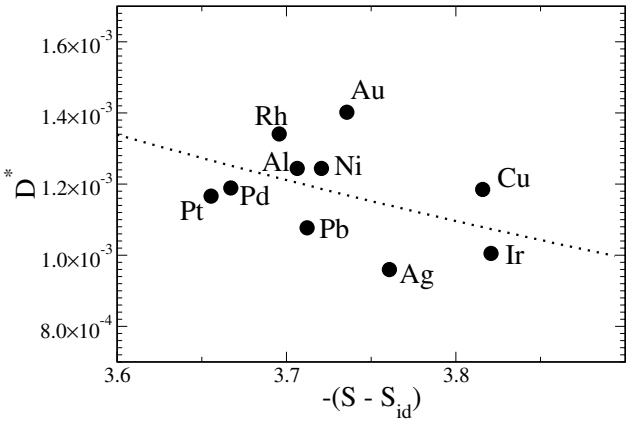

Figure 4. Scaled diffusion coefficients for the liquid phase at the calculated melting temperature, for the different elements considered in this study, versus excess entropy. The dotted line corresponds to Dzugutov's universal scaling relation [55].

4. Conclusions

We have reported results from an extensive study of the melting and thermodynamic properties of a series of fcc metals modelled with the potentials proposed by Cleri and Rosato [13]; in the case of Pb, we have compared this potential with the 'glue' model of Lim *et al* [14]. We have found that both models tend to underestimate the melting temperature of fcc metals by as much as 30%, which implies a difference of almost 600 K in the case of Pd with respect to the experimental value, or 400 K in the case of Au. The trend to underestimate is broken in the cases of Ir and Rh, for which there is an overestimation of 20%. While these discrepancies may seem large, it should be pointed out that the form of the potential is very simple, and that, in its construction and fitting, no information on the thermal properties of the metals, nor on their liquid phase, are included. Taking this observation into account, it is remarkable that at least melting trends among the different metals seem to be correctly reproduced. Other melting properties, such as fusion enthalpies and entropies, fractional volume changes and the pressure derivative of the melting line at zero pressure ($\mathrm{d}T_\mathrm{f}/\mathrm{d}P$), are reproduced with varying degrees of success, but generally within $\pm 30\%$ of the experimental value. For the particular cases of Al and Cu, where the calculated $\mathrm{d}T_\mathrm{f}/\mathrm{d}P$ value is in reasonable agreement with the experimental values, we have also calculated the melting line predicted by the model up to 20 GPa.

Concerning transport properties such as the diffusivity and the viscosity of the molten metals, we have found values which are consistent with both the available experimental data and results from previous theoretical work [59]. Our calculated diffusion constants at melting for the liquid phase are consistent with Dzugutov's universal relation.

Acknowledgments

We acknowledge financial support from the Spanish Ministry of Science and Education through project BFM2003-03372-C03-03, and from the Catalan Regional Government through project 2005SGR683. The use of computational facilities at CESCA (Catalunya), CESGA (Galicia) and ICM (University of Warsaw) is gratefully acknowledged.

References

[1] Gale W F and Totemeir T C (ed) 2003 *Smithells Metals Reference Book* 8th edn (USA: Elsevier Butterworth-Heinemann)
[2] Young D A 1992 *Phase Diagrams of the Elements* (Berkeley, CA: University of California Press)

[3] Laio A, Bernard S, Chiarotti G L, Scandolo S and Tosatti E 2000 *Science* **287** 1027
[4] Belonoshko A B, Ahuja R and Johansson B 2000 *Phys. Rev. Lett.* **84** 3638
[5] Belonoshko A B, Ahuja R, Eriksson O and Johansson B 2000 *Phys. Rev.* B **61** 3838
[6] Broughton J Q and Li X P 1987 *Phys. Rev.* B **35** 9120
[7] Cook S J and Clancy P 1993 *Phys. Rev.* B **47** 7686
[8] Keblinski P, Bazant M Z, Dash R K and Treacy M M 2002 *Phys. Rev.* B **66** 064104
[9] Kaczmarski M, Rurali R and Hernández E 2004 *Phys. Rev.* B **69** 214105
[10] Kaczmarski M, Bedoya-Martínez O N and Hernández E R 2005 *Phys. Rev. Lett.* **94** 095701
[11] Ghiringhelli L M, Los J H, Meijer E J, Fasolino A and Frenkel D 2005 *Phys. Rev. Lett.* **94** 145701
[12] Lee B J, Shim J H and Baskes M I 2003 *Phys. Rev.* B **68** 144112
[13] Cleri F and Rosato V 1993 *Phys. Rev.* B **48** 22
[14] Lim H S, Ong C K and Ercolessi F 1992 *Surf. Sci.* **270** 1109
[15] Ducastelle F 1970 *J. Physique* **31** 1055
[16] Ducastelle F and Cyrot-Lackmann F 1970 *J. Phys. Chem. Solids* **31** 1295
[17] Holender J M 1990 *Phys. Rev.* B **41** 8054
[18] Gómez L, Dobry A and Diep H T 1997 *Phys. Rev.* B **55** 6265
[19] Laio A and Parrinello M 2002 *Proc. Natl Acad. Sci. USA* **99** 12562
[20] Martoňák R, Laio A and Parrinello M 2004 *Phys. Rev. Lett.* **90** 075503
[21] Oganov A R, Martoňák R, Laio A, Raiteri P and Parrinello M 2005 *Nature* **438** 1142
[22] Wilson M and McMillan P F 2003 *Phys. Rev. Lett.* **93** 135703
[23] Alfè D 2003 *Phys. Rev.* B **68** 064423
[24] Bonev S A, Schwegler E, Ogitsu T and Galli G 2004 *Nature* **431** 669
[25] Johnson J K, Zollweg J A and Gubbins K E 1993 *Mol. Phys.* **78** 591
[26] Watanabe M and Reinhardt W P 1990 *Phys. Rev. Lett.* **65** 3301
[27] de Koning M, Antonelli A and Yip S 1999 *Phys. Rev. Lett.* **83** 3973
[28] de Koning M, Antonelli A and Yip S 2001 *J. Chem. Phys.* **115** 11025
[29] Bond S D, Leimkuhler B J and Laird B B 1999 *J. Comput. Phys.* **151** 114
[30] Andersen H C 1980 *J. Chem. Phys.* **72** 2384
[31] Souza I and Martins J L 1997 *Phys. Rev.* B **55** 8733
[32] Hernández E 2003 *J. Chem. Phys.* **115** 10282
[33] Rurali R and Hernández E 2003 *Comput. Mater. Sci.* **28** 85
[34] *CRC Handbook of Chemistry and Physics* 2004 84th edn (Boca Raton, FL: CRC Press)
[35] Vočadlo L, Alfè D, Price G D and Gillan M J 2004 *J. Chem. Phys.* **120** 2872
[36] de Wijs G A, Kresse G and Gillan M J 1998 *Phys. Rev.* B **57** 8223
[37] Vočadlo L and Alfè D 2002 *Phys. Rev.* B **65** 214105
[38] Lindemann F A 1910 *Z. Phys.* **11** 609
[39] Dash J G 1999 *Rev. Mod. Phys.* **71** 1737
[40] Born M 1939 *J. Chem. Phys.* **7** 591
[41] Jin K L Z H, Gumbsch P and Ma E 2001 *Phys. Rev. Lett.* **87** 055703
[42] Martin C J and O'Connor D A 1977 *J. Phys. C: Solid State Phys.* **10** 3521
[43] Jesson B J and Madden P A 2000 *J. Chem. Phys.* **113** 5924
[44] Cannon J F 1974 *J. Phys. Chem. Ref. Data* **3** 781
[45] Hänström A and Lazor P 2000 *J. Alloys Compounds* **305** 209
[46] Mirwald P W and Kennedy G C 1979 *J. Geophys. Res.* **84** 6750
[47] Chase M W, Davies C A, Downey J R, Frurip D J, Mcdonald R A and Syverud A N 1985 *J. Phys. Chem. Ref. Data Suppl.* **14** 1
[48] Turnbull D 1950 *J. Appl. Phys.* **21** 1022
[49] Strong H M and Bundy F P 1959 *Phys. Rev.* **115** 278
[50] Mirwald P W and Kennedy G C 1976 *J. Phys. Chem. Solids* **37** 795
[51] Boehler R and Ross M 1997 *Earth Planet. Sci. Lett.* **153** 223
[52] Moriarty J A 1986 *Shock Waves in Condensed Matter* vol 101, ed Y M Gupta (New York: Plenum)
[53] Rosenfeld Y 1977 *Phys. Rev.* A **15** 2545
[54] Rosenfeld Y 1999 *J. Phys.: Condens. Matter* **11** 5415
[55] Dzugutov M 1996 *Nature* **381** 137
[56] Hoyt J J, Asta M and Sadigh B 2000 *Phys. Rev. Lett.* **85** 594
[57] Li G X, Liu C S and Zhu Z G 2005 *Phys. Rev.* B **71** 094209
[58] Alfè D and Gillan M J 1998 *Phys. Rev. Lett.* **81** 5161
[59] Alemany M M G, Diéguez O, Rey C and Gallego L J 1999 *Phys. Rev.* B **60** 9208